Available online at www.sciencedirect.com
SCIENCE DIRECT®
Physica D 180 (2003) 1–16
PHYSICA D
www.elsevier.com/locate/physd

How fast elements can affect slow dynamics

Koichi Fujimoto*, Kunihiko Kaneko

Department of Pure and Applied Sciences, Graduate school of Arts and Sciences, University of Tokyo, 3-8-1, Komaba, Meguro, Tokyo 153-8902, Japan

Received 27 June 2002; received in revised form 22 December 2002; accepted 18 January 2003
Communicated by Y. Kuramoto

Abstract

A chain of coupled chaotic elements with different time scales is studied. In contrast with the adiabatic approximation, we find that correlations between elements are transferred from faster to slower elements when the differences in the time scales of the elements lie within a certain range. For such correlations to occur, three features are essential: strong correlations among the elements, a bifurcation in the dynamics of the fastest element by changing its control parameter, and cascade propagation of the bifurcation. By studying coupled Rössler equations, we demonstrate that fast elements can affect the dynamics of slow elements when these conditions are satisfied. The relevance of our results to biological memory is briefly discussed.

PACS: 05.45.−a; 05.45.Xt; 05.45.Jn; 89.75.−k

Keywords: Multi time scale dynamics; Bifurcation cascade; Chaos; Frequency locking

1. Introduction

Many biological, geophysical and physical problems include a variety of modes with different time scales. In biological rhythms, dynamics with time scales as long as a day can be organized through biochemical reactions occurring on subsecond time scales. In the brain, fast sensory inputs are successively transferred to dynamics with longer time scales, and are stored from short-term memory to long-term memory. Since memory should last longer than the time scale of external stimuli, some mechanism to embed change at faster time scales into events at much slower time scales is required. The study of dynamical systems with various time scales is important for understanding the hierarchical organization of such systems by investigating the dynamic interactions among modes.

Adiabatic elimination [1] is often adopted for systems with different time scales. If the correlations between modes with different scales are neglected, the fast variables are eliminated and the dynamics of the system is expressed only by the slow variables. The fast variables are then replaced by their averages and noise. In this adiabatic approximation, the characteristics of the dynamics of the fast time scales disappear, and influence of fast variables on slow variables is only retained as memory terms in the Langevin equation.

* Corresponding author.
E-mail address: fujimoto@complex.c.u-tokyo.ac.jp (K. Fujimoto).

0167-2789/03/$ – see front matter © 2003 Elsevier Science B.V. All rights reserved.
doi:10.1016/S0167-2789(03)00046-0

The adiabatic approximation is valid when the differences between the time scales are large. However, when the differences are small, correlations between the modes appear, invalidating the approximation. In this case, the fast scale dynamics can influence the dynamics of the slower variables. Here we investigate under what conditions the faster variables can influence the dynamics of the slower variables. We will show that from change of fast dynamics is propagated to slow dynamics, but not from slow to fast dynamics, when a certain condition is satisfied. Chaos is relevant to this since chaos makes the amplification of microscopic perturbations to a macroscopic scale possible. On the other hand, the existence of chaos disturbs the correlations between the two variables of different time scales. In order for the propagation of statistical properties from fast to slow variables to occur, it turns out that two other properties are required: strong correlation (with partial coherence) and a cascade of bifurcations.

In the present paper, we investigate the dynamical behavior of high dimensional systems where spatiotemporal chaos with a cascade of bifurcations is found to be caused by interactions among different time scales and its relevance to the flow of perturbation from fast to slow elements. In Section 2, a model of coupled chaotic elements with different time scales is introduced. In Section 3, the Rössler equation is adopted as the basic unit chaotic oscillator. Elements at slower time scales are found to exhibit bifurcations influenced by the bifurcations of the faster elements. A cascade of bifurcations, transferred successively from fast to slow elements, is reported through the analysis of the power spectrum and the phase space structure. In Section 4, the cascade is shown to appear in some range of the time scale difference. In Section 5 we study the conditions for the occurrence of the bifurcation cascade and characterize them. Section 6 is devoted to the discussion and the conclusion.

2. Model

2.1. Coupled oscillator with different time scales

In the present paper, we investigate how statistical (topological) properties of slow dynamics can depend on those of the fast dynamics by studying a coupled dynamical system with different time scales. To be specific, we choose a chain of nonlinear oscillators whose typical time scales are distributed as a power series. The dynamics of each oscillator is assumed to differ only in its time scale, and thus there are only three control parameters in our model: one for the nonlinearity, one for the coupling strength among oscillators, and one for the difference in time scales.

The concrete form adopted here is as follows. We choose a nonlinear differential equation as the single oscillator. The time scale differences are introduced as

$$T_i \frac{\mathrm{d}\vec{X}_i}{\mathrm{d}t} = \vec{F}(\vec{X}_i), \quad T_i \equiv T_1 \tau^{i-1}. \tag{1}$$

The index of the elements is denoted by i with $i = 1, 2, \ldots, L =$ system size. T_i is the characteristic time scale for each element and τ (<1) is the time scale difference. By adopting a power series distribution for the characteristic time scales, the relationship between any element i and $i+1$ is identical, as is easily checked by scaling the time t by T_i in each equation. Hence this form is useful for studying the relevance of time scale change, since the dynamics of each element, after rescaling the time, is identical. Note also that this is analogous to the shell model of turbulence [2]. The total time scale difference is given by

$$T_{\text{total}} \equiv \frac{T_L}{T_1} = \tau^{L-1}. \tag{2}$$

In the present paper, we adopt τ as a control parameter by fixing $T_{\text{total}} = 100$ and change L accordingly following Eq. (2) couple neighboring elements. The Runge–Kutta method was used with a time step size such that the fastest element $\vec{X}_i$ is computed with a high precision.

Next, we need some coupling term among elements. Here we choose the nearest-neighbor coupling, given from the function of $\Delta\vec{X}_i \equiv \vec{X}_{i+1} + \vec{X}_{i-1} - 2\vec{X}_i$. Often linear diffusion coupling given by just the term $\Delta\vec{X}_i$ is adopted for couplings. As far as we have examined, the behavior to be reported is not observed in the linear diffusion coupling term. Some mode couplings are necessary. Then, as a next step, nonlinear coupling up to the quadratic term is considered, including the terms $X_i^k \Delta X_i^m$ and $\Delta X_i^k\ \Delta X_i^m$ (with X_i^k as the kth component of $\vec{X}_i$ order). The behavior to be reported is observed in a wide range of models (as long as this coupling term does not bring about the divergence of orbits). Here we take an example of Rössler equation, and study some models with such couplings.

In fact, nonlinear couplings among modes are not so usual. By expanding nonlinear partial differential equation with the evolution of spatial Fourier modes, nonlinear couplings commonly appear. For example, coupled ordinary differential equations with nonlinear couplings is derived from Navier–Stokes and heat equations, having a larger number of modes than Lorenz equation [3,4].

As for the boundary condition we choose free boundary condition at $i = 1$ and L, but this specific choice is not important.

2.2. Specific model: coupled Rössler equations

As a specific example, we choose the Rössler equation as the single oscillator:

$$\dot{x} = f_x(\vec{X}) \equiv -y - z, \qquad \dot{y} = f_y(\vec{X}) \equiv x + ay, \qquad \dot{z} = f_z(\vec{X}) \equiv bx - rz + xz. \tag{3}$$

$\vec{X} \equiv (X^1, X^2, X^3) \equiv (x, y, z)$ denotes the variables of each element.[1] The parameters a and b are fixed at 0.36 and 0.4, respectively, whereas r is a control parameter.

Here we choose the coupling with the neighboring elements as follows:

$$\begin{aligned} T_i\dot{x}_i &= f_x(\vec{X}_i) + \sum_j d_{1j}^d \Delta X_i^j, \qquad T_i\dot{y}_i = f_y(\vec{X}_i) + \sum_j d_{2j}^d \Delta X_i^j, \\ T_i\dot{z}_i &= f_z(\vec{X}_i) + \sum_j d_{3j}^d \Delta X_i^j + d_1^n z_i \Delta x_i + d_2^n x_i \Delta z_i + d_3^n \Delta x_i \Delta z_i. \end{aligned} \tag{4}$$

As a nonlinear coupling here we choose only the terms related with xz, for the change of z, since the original equation involves only such nonlinear coupling. This nonlinear coupling term introduces nonlinear interaction term between the modes of the neighboring elements.

This choice of coupling is mainly adopted to avoid the divergence of orbits. (By including other nonlinear coupling terms which the original Eq. (3) do not contain (for example, $x_i x_{i+1}$, $y_i y_{i+1}$, and $z_i z_{i+1}$), variables of the resultant coupled system easily diverge.) On the other hand, nonlinear coupling terms are necessary for the phenomena to be reported here. Hence, as a simple choice of nonlinear coupling term, we take only the nonlinear coupling that exists in the original equations.

Still, there remain arbitrary choices of coupling terms. We have studied several examples, and the results to be reported are commonly observed by choosing the coupling parameter values suitably. As a specific example, we report the results obtained using the following coupling:

$$\mathbf{D^d} \equiv \begin{bmatrix} d_{11}^d & d_{12}^d & d_{13}^d \\ d_{21}^d & d_{22}^d & d_{23}^d \\ d_{31}^d & d_{32}^d & d_{33}^d \end{bmatrix} = d_d \begin{bmatrix} 0 & -1 & 0 \\ 1 & a & 0 \\ b & 0 & 0 \end{bmatrix}, \qquad d_2^n = d_3^n = 0. \tag{5}$$

[1] Since the choice of the variables x, y, z is usual for Rössler equation, we use this notation, but for the convenience of vector representation we also use X^j.

There, the nonlinear coupling terms are $z_i x_{i+1}$ and $z_i x_{i-1}$. (The phenomena reported below appears in the wide range of the coupling strength, for example, $d_1^n \geq 0.25$ under $d_d = 0.4$, $(\tau, L) = (1.93, 8)$ and $r = 1.4$ in Eqs. (4) and (5).)

In this model, absence of divergence is expected from the following argument. With $d_1^n = d_d = (d/2)$, Eqs. (5) and (4) is transformed into

$$T_i \frac{\mathrm{d}\vec{X}_i}{\mathrm{d}t} = \vec{F}((\mathbf{E} - \mathbf{D})\vec{X}_i + \tfrac{1}{2}\mathbf{D}(\vec{X}_{i-1} + \vec{X}_{i+1})), \tag{6}$$

$$\mathbf{D} = \begin{bmatrix} d_x & 0 & 0 \\ 0 & d_y & 0 \\ 0 & 0 & d_z \end{bmatrix}, \quad \mathbf{E} = \begin{bmatrix} 1 & 0 & 0 \\ 0 & 1 & 0 \\ 0 & 0 & 1 \end{bmatrix},$$

where $d_z = 0$ and $d_x = d_y = d = 0.45$ in the following simulations. [2] Since in the original equation $(\mathrm{d}\vec{X}_i/\mathrm{d}t) = \vec{F}(\vec{X}_i)$, the orbits do not diverge (for suitable initial conditions), the stability of the coupled system is also assured. As mentioned, this specific choice is not important. See Appendix A for another example showing the phenomena to be reported.

3. Transfer of correlation from fast to slow elements in coupled Rössler equations

3.1. Frequency locking in the case with small difference in time scales

As a preparation for the later study, we briefly describe a property of a system with two elements, that are fast and slow. With this, we discuss a basic condition for propagation of correlation from fast to slow elements. First, some correlations between pairs of elements are required to be propagated. This correlation exists, when the difference in the time scales between the two elements is not so large.

As a typical example with such correlation, we study the case with frequency locking between two elements (or, pairs of nearest-neighbor elements since these have the closest time scales). Examples of $x_i(t)$ time series are shown in Fig. 1(a), where we have taken $(\tau, L) = (1.93, 8)$. The corresponding power spectrum[3] of each element is shown in Fig. 1(b), where one can detect some common peaks among elements. These figures show that there are fixed relations between peaks, in other words frequency locking between elements. The relationship of frequencies of the two elements is not necessarily by 1:1 frequency relationship but generally with $n : m$ (with $m > n$), between neighboring elements. In the example of the figure, the phase lockings between the two elements range from 1:1,

[2] By introducing $\vec{W}_i$ as

$$\vec{W}_i \equiv (\mathbf{E} - \mathbf{D})\vec{X}_i + \tfrac{1}{2}\mathbf{D}(\vec{X}_{i-1} + \vec{X}_{i+1}).$$

Eq. (6) is transformed into

$$\frac{\mathrm{d}\vec{W}_i}{\mathrm{d}t} = (\mathbf{E} - \mathbf{D})\frac{\vec{F}(\vec{W}_i)}{T_i} + \frac{\mathbf{D}}{2}\frac{\vec{F}(\vec{W}_{i+1})}{T_{i+1}} + \frac{\mathbf{D}}{2}\frac{\vec{F}(\vec{W}_{i-1})}{T_{i-1}}.$$

In the present model Eq. (4), we adopted the coupling parameters and $d_1^n = d_d = (d/2)$, $d_z = 0$ and $d_x = d_y$. Then all the coupling terms in Eq. (4) are represented by linear terms of $\vec{W}_i$, because of $d_z = 0$. This is close to usual diffusion coupling, but the coupling strength is asymmetric since $T_{i+1} > T_{i-1}$.

[3] Since the range of frequency in the dynamics differ by the element i, we set the sampling time for the power spectrum as kT_i with k a given constant.

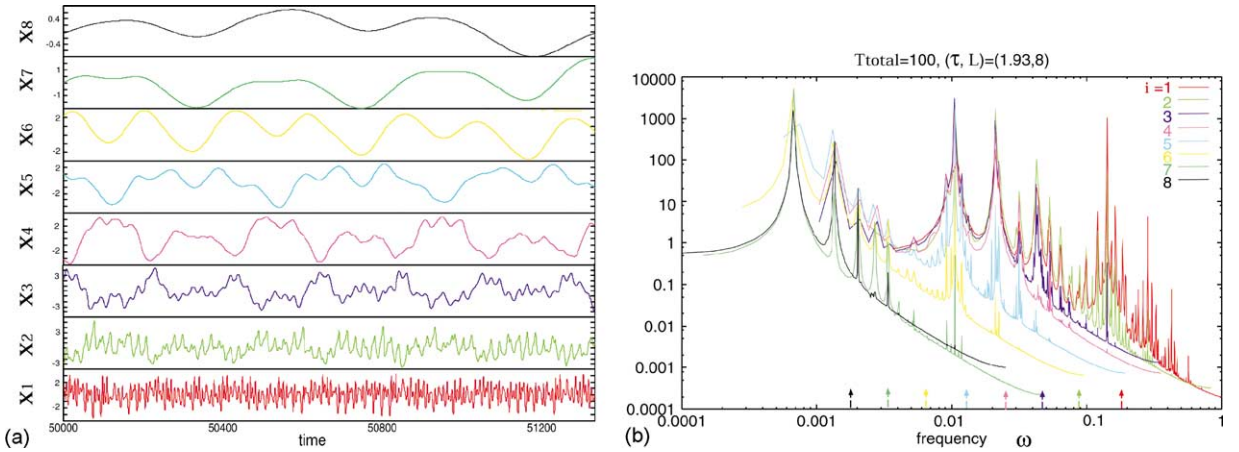

Fig. 1. (a) Time series of $x_i(t)$. (b) The power spectrum of $x_i(t)$. $(\tau, L) = (1.93, 8)$ and $r = 1.4$. (a) shows correlated motion occurring among the neighboring elements with various time scales. The colors correspond to the different elements, whereas (b) shows some common peaks corresponding to the frequency locking. The arrows on the x-axis indicate the basic frequency of each element there is no coupling ($d = 0$).

2:3, and to 1:2, approximately. As in the case of coupled phase oscillators with different frequencies [5,6], the frequency locking appears, as long as the time scale difference τ is not too large and coupling strength not too weak. As long as the coupling between two elements is not too small, this frequency locking is observed at various time scales.

The co-variance between two elements, given by $(\langle(x_i-\langle x_i\rangle)(x_{i+1}-\langle x_{i+1}\rangle)\rangle/\sqrt{\langle(x_i-\langle x_i\rangle)^2\rangle\langle(x_{i+1}-\langle x_{i+1}\rangle)^2\rangle})$, takes a large value[4]. The correlation between the elements, however, decays rather rapidly as the distance between the elements (i.e., the difference between their time scales) increases. For example, the co-variance between the fastest and slowest elements, given by $(\langle(x_1-\langle x_1\rangle)(x_L-\langle x_L\rangle)\rangle/\sqrt{\langle(x_1-\langle x_1\rangle)^2\rangle\langle(x_L-\langle x_L\rangle)^2\rangle})$, takes almost zero values. This is not surprising, since the motion here is chaotic and the correlation decays due to the chaotic instability.

Note that in the present model with strong coupling strength and small time scale difference τ, as exhibited in Fig. 1, chaos appears at $r = 1.4$ where the single Rössler equation still exhibits a limit cycle. (The bifurcation from a limit cycle to chaos occurs at $r = r_c^R \sim 3.45$ for a single Rössler equation.)

3.2. *The response of the slow dynamics to change in the fastest element*

Now we will study how some change in one element can be transferred to others with different time scales. In order to check this generally, we need to study how some input applied to a given element influences dynamics of other elements. For it we set up the following external operation, and study the response.

External operation and response. After the initial transients have died out, at an arbitrarily chosen point in the temporal evolution, we apply $A \sin(t/T_0)$ at a given element i, where the time scale T_0 is the order of that of the element ($T_0 \sim T_i$). Then we examine if this addition of an external input to a given element influences the dynamics of other elements with different time scale.

Here, we will show that the slowest dynamics at $i = L$ can be influenced by the fastest element at $i = 1$. Hence, we apply an input at the fastest mode $i = L$ and see if it influences the dynamics of the slowest mode at $i = L$. As

[4] $\langle\cdots\rangle$ denotes the ensemble average.

a measure for the dynamics of $x_L(t)$, we first adopt the power spectra $x_i(t)$, and see if the spectra at the point $i = L$ are altered by the application of an external input at $i = 1$.

Fig. 2 shows the power spectra of the slowest element $i = L$, where the external input described above applied at the fastest element $i = 1$. Each figure shows the spectra for the slowest element x_L, for a choice of different (τ, L), while the total difference $T_{\text{total}} = \tau^{L-1}$ is fixed. Lines with different colors correspond to the spectra with an input of different periods as well as those without input.

To be specific, we have plotted the power spectra for the slowest element x_L, with $T_{\text{total}} = 100$, for $(\tau, L) = (100, 2)$ (a), $(4.64, 4)$ (b), $(2.51, 6)$ (c), $(1.93, 8)$ (d), $(1.67, 10)$ (e), $(1.27, 20)$ (f). The black line shows the power spectrum without $i = 1$ input periods, while the other colors give the spectra obtained for an input with different periods $T_0 = 1.5$ (red), 1.1 (blue), and 0.7 (green), applied at $i = 1$.

Now it is clear that the spectra of the slowest element are altered for the case (c) and (d), and weakly for (e), while other data show little or almost no change in the spectra. The power spectrum of the slowest element depends on the input period T_0 for the cases (c)–(e).

The propagation of influence to slower elements reported here is possible within a range of (τ, L). Consider the transfer to an element with a given time scale difference T_{total}. Then each time scale difference τ and the number of elements satisfies $T_{\text{total}} = \tau^{L-1}$. Here the propagation to the slowest element is possible only within a given range of τ. If τ is small, the propagation of influence decays at some element, since L is large. If τ is large, on the other hand, the correlation of elements is too weak to support the propagation. (A detailed mechanism for the propagation will be discussed in Section 5 as bifurcation cascade, while a quantitative condition on (τ, L) for the propagation will be shown in Section 4.)

3.3. *Dynamics in the intermediate time scales*

Now we study, how a change in the fastest element is transferred to the slowest element. To make such propagation possible, the change has to be transferred to the neighboring element step by step. Hence we study how the dynamics of all elements are correlated by plotting the power spectrum of all of $x_i(t)$. In Fig. 3, the spectra of $x_i(t)$ are plotted for input with period $T_0 = 1.1$ (a) and 1.5 (b) with $A = 0.5$. Here $T_{\text{total}} = 100$ and $(\tau, L) = (1.93, 8)$. As already mentioned there are common peaks in the spectra. Compared with Fig. 1(b), the spectrum of the slow element represented by the black line shows a shift in the peak frequency in (a) while a broad spectrum (as a signature of bifurcation to chaos) is observed in (b). Here peaks after the input are shifted keeping the agreement between elements. Hence, the dynamics of the slowest element are altered element by element, according the change of the fastest element.

To see more closely the change of the dynamics, direct observation of an orbit of each element in the phase space is relevant. Here we detect the change of dynamics by plotting the Poincaré map, corresponding to Figs. 1 and 3.

Fig. 4 shows the T_0 dependence of the Poincaré section sliced at $\dot{y}_i = 0$. Different colors give the plots for without external inputs, and with input $A \sin(t/T_0)$ with $T_0 = 1.5$ and 1.1, applied to the fastest element $i = 0$. For $A = 0$, almost all the elements, ranging from the fast to the slow time scales, show weakly chaotic dynamics or multiple tori near the onset of chaos, as shown by the black dots. For $A = 0.5$ and $T_0 = 1.1$, nonchaotic (limit cycle or tori) dynamics are observed as shown by the blue dots, while strongly chaotic dynamics appear for $A = 0.5$ and $T_0 = 1.5$ as shown by the red dots. Therefore the input $A \sin(t/T_0)$ applied to, and causing a bifurcation in the fastest element induces a bifurcation of the slowest dynamics also. Hence the dynamics of the slowest element are altered by the application of an input to the fastest element. We call this bifurcation transfer a "bifurcation cascade".

This bifurcation cascade can also be induced by changing the control parameter r of $i = 1$, instead of adding the external input. Again, if the parameter of the fastest element is changed so that that element shows a bifurcation, then the slowest elements also show the bifurcation. Therefore, in both cases, by inducing a bifurcation in the fastest

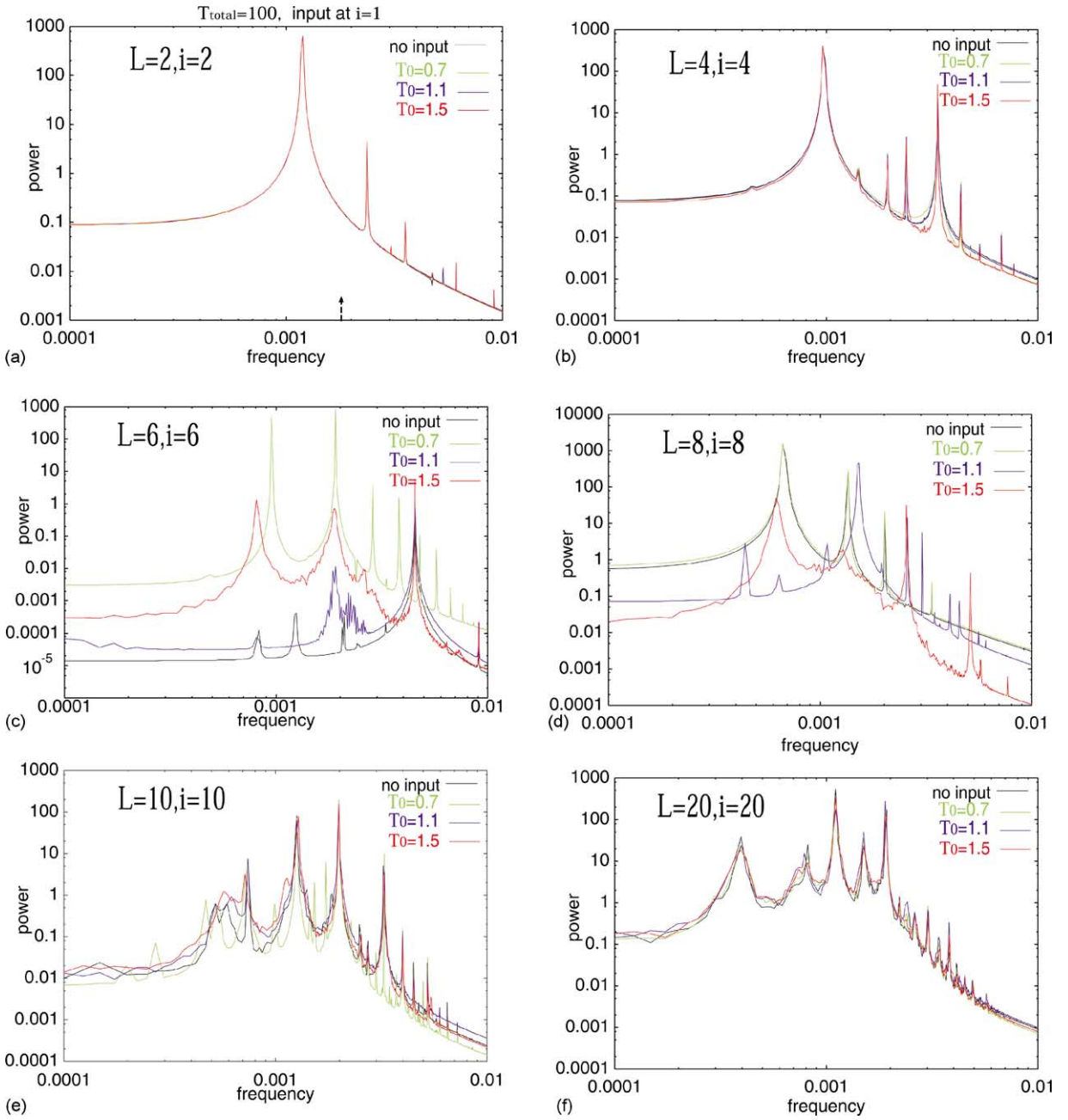

Fig. 2. Power spectra for the slowest element x_L, with $T_{\text{total}} = 100$, for $(\tau, L) = (100, 2)$ (a), (4.64, 4) (b), (2.51, 6) (c), (1.93, 8) (d), (1.67, 10) (e), (1.27, 20) (f). The black line gives the x_L spectra without any input at element $i = 1$ while the other colors give the spectra with various input periods: $T_0 = 1.5$ (red), 1.1 (blue), and 0.7 (green), applied at $i = 1$ with $A = 0.5$. The dependence on T_0 appears only in (c)–(e), For the other cases, the power spectra are not influenced by the application of the input to the fastest element. The arrow on the x-axis in (a) indicates the basic frequency of the slowest element there is no coupling ($d = 0$).

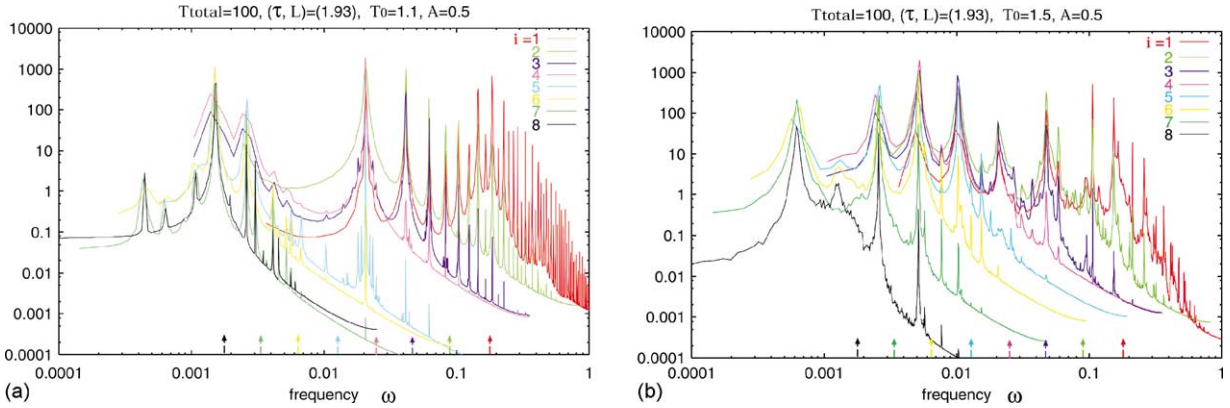

Fig. 3. Power spectrum for $x_i(t)$, when the input $A \sin(t/T_0)$ is applied at $i = 1$ ($T_0 \sim T_1$), where $T_0 = 1.1$ (a), 1.5 (b), and $A = 0.5$. The spectra for different elements are plotted in different colors. In both the spectra of the slowest element represented by the black line is shifted due to the input, keeping the agreement of peaks of faster elements. The arrows on the x-axis indicate the basic frequency of each element there is no coupling ($d = 0$).

element, it is transferred to the slowest element successively through a bifurcation cascade. Actually, when the change of parameters or addition of the inputs do not lead to the bifurcation of the fastest element but its continuous change, this influence is not transferred to the slowest element.

Here we come back to the question why the change is not induced at the slowest element when τ is large as given in Fig. 2(f). In this case, due to large time scale difference, the correlation of neighboring elements is so weak that the bifurcation at one element is not propagated to the next. Thus the bifurcation cascade does not appear.

3.4. Asymmetry of the bifurcation cascade

So far we have shown that the slower elements are successively influenced by the faster elements. Now we study the opposite case, i.e., the influence of the faster elements by the change of slower elements. We will show that the fastest dynamics at $i = 1$ cannot be influenced by the slowest element at $i = L$, in contrast to the influence of the bifurcation of the fastest element on the slowest one discussed in the last subsection.

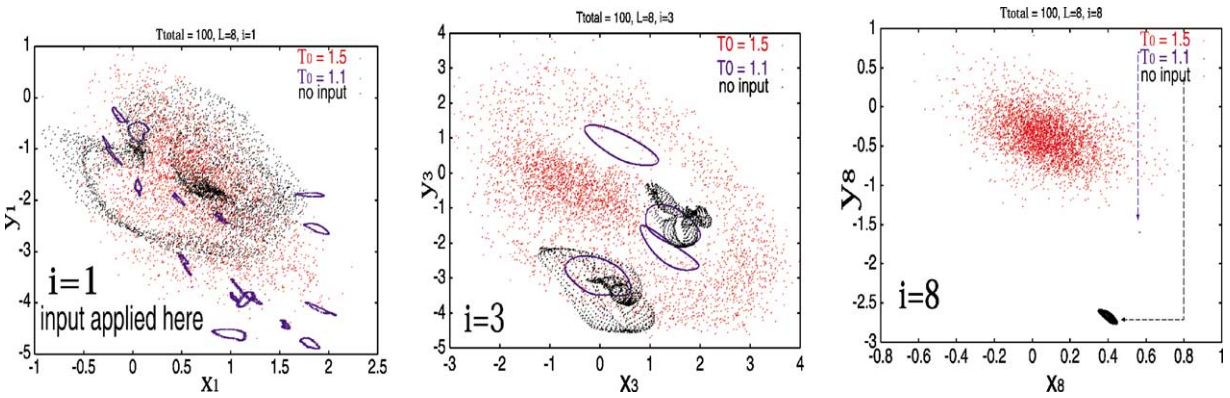

Fig. 4. Poincaré plots of (x_i, y_i) sliced at $\dot{y}_i = 0$ are shown for $i = 1, 3, 8$. The input $A \sin(t/T_0)$ is applied to the fastest element $i = 0$ where $(\tau, L) = (1.93, 8)$ and $T_{\text{total}} = 100$. The black dots show the results for $A = 0$, the same time series as used in Fig. 1, while the red dots show results for $T_0 = 1.5$, and the blue dots for $T_0 = 1.1$, with $A = 0.5$, the same parameters as used in Fig. 3.

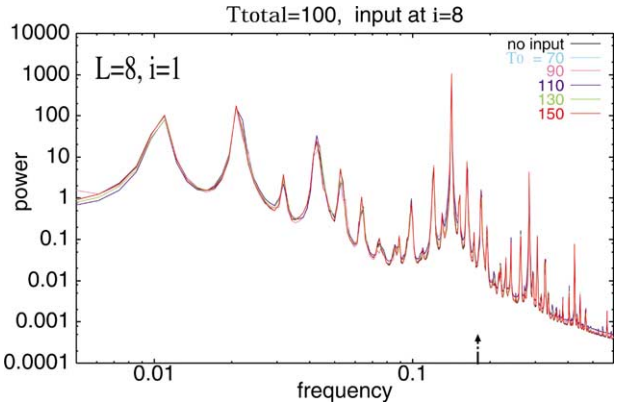

Fig. 5. Power spectrum of the fastest element x_1, with $T_{\text{total}} = 100$, $(\tau, L) = (1.93, 8)$. The black line gives the spectra without any input at $i = L$ while the other colors give the spectra with input of period $T_0 = 150$ (red), 130 (green), 110 (blue), 90 (pink), and 70 (sky blue), applied at $i = L$. $A = 0.5$. The arrow on the x-axis indicates the basic frequency of the fastest element there is no coupling ($d = 0$).

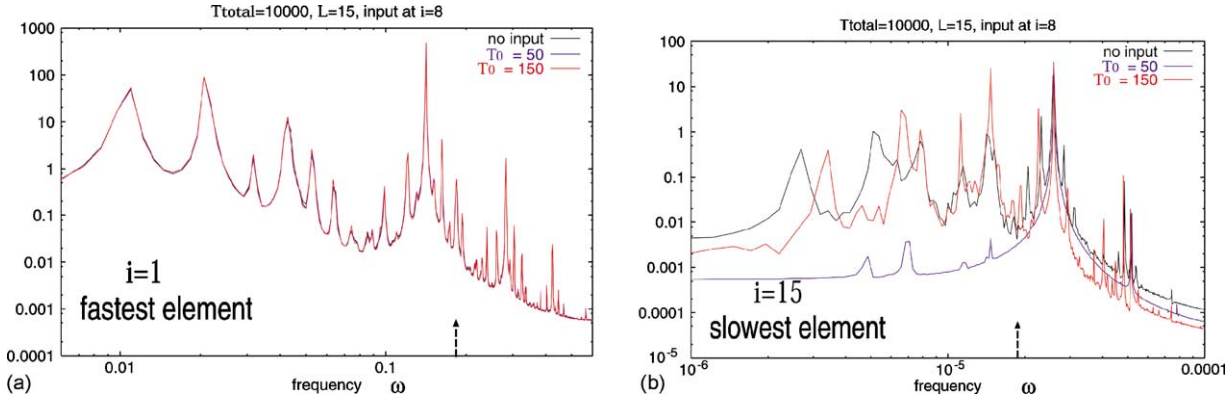

Fig. 6. Power spectrum at $i = 1$ (a) and $i = L$ (b), where the input is applied at the intermediate element, $i = (L + 1)/2$ with $T_i = \sqrt{T_{\text{total}}}$. The colors correspond to the input period $T_0 \sim T_{(L+1)/2}$ same as Fig. 7. $L = 15$, $T_{\text{total}} = 10\,000$ with same τ in $L = 8$, $T_{\text{total}} = 100$. The arrows on the x-axis indicate the basic frequency of each element there is no coupling ($d = 0$).

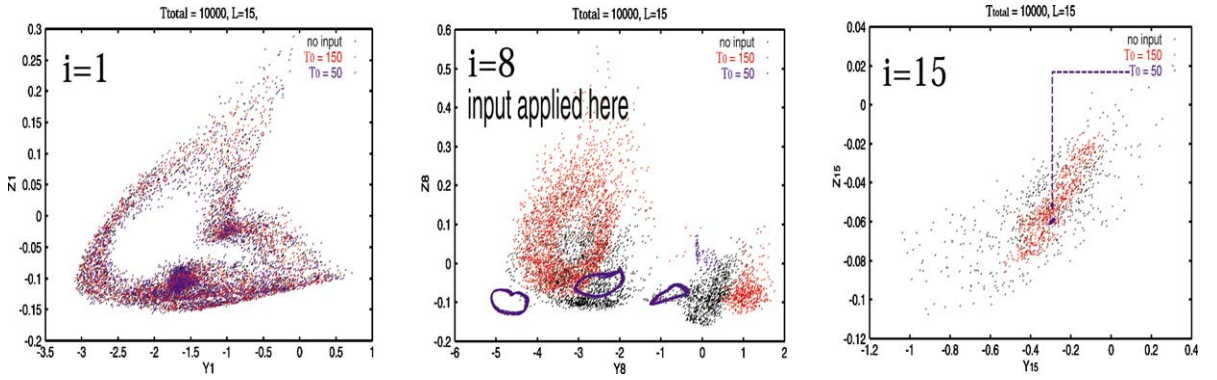

Fig. 7. Poincaré section sliced at $x_i(t) = 0$, where the input $A \sin(t/T_0)$ is applied at the intermediate element $i = 8$ with $(\tau, L) = (1.93, 15)$ and $T_{\text{total}} = 10^4$. Black points give the Poincaré plot for $A = 0$ while the red points give the plot for the input period $T_0 = 150$, and the blue for $T_0 = 50$, with $A = 0.5$. The input dependence appears at the slowest element $i = L$ but not at the fastest one $i = 1$.

In order to check this, we have carried out the external operation given in Section 3.2. But instead of applying the input to the fastest element, we apply the input $A \sin(t/T_0)$ at the slowest element $i = L$ ($T_0 \sim T_L$). Then we examine how this influences the fastest dynamics at $i = 1$.

Here we choose the same model parameters as in 3.2, and again study the change of the power spectra by the addition of the input. Fig. 5 shows the power spectra of the fastest element $x_1(t)$ depending on the input with different period T_0, as plotted by a different color, for $(\tau, L) = (1.93, 8)$. As shown, no input dependence appears for the fastest element. This is true in general for $L \geq 3$. (For $L = 2$, there is direct, slight influence to the next element as explained by adiabatic approximation.)

To sum up, the fast dynamics are not affected by the slowest element for any range of τ. By comparing Figs. 2 and 5, one can see that the bifurcation cascade can be transmitted from the fast to slow elements but not from the slow to fast elements. To further confirm this asymmetry, we have carried out the following numerical experiment.

Instead of the input at the fastest or slowest element so far, we apply the input $A \sin(t/T_0)$ at the middle element $i = (L + 1/2)$, after the initial transients have died out. (Recall that the time scale difference $T_0 \sim T_{(L+1/2)} = \sqrt{T_{\text{total}}}$.) Then we examine how this input to the middle element influences both the fast dynamics at $i = 1$ and the slow dynamics at $i = L$.

Here we show an example by adopting the same parameter values, and the same τ value (i.e., 1.93) as for Figs. 2(d) and 5. The system size is set at $L = 15$, i.e., $T_{\text{total}} = \tau^{L-1} = 10\,000$.

Fig. 6 shows how the corresponding power spectra of $i = 1$ (a) and $i = L$ (b) depend on the input when the input is applied at the intermediate element. Now, the dependence appears only in the slow dynamics, $i = L$, but not at $i = 1$ as in Fig. 7.

Fig. 7 shows the Poincaré plot sliced at $x_i(t) = 0$, where the input $A \sin(t/T_0)$ is applied at the intermediate element with $T_i = \sqrt{T_{\text{total}}}$. The meaning of the colors is explained in the figure. As can be seen, the input dependence is blurred in the faster elements but is clearly discernible in the slower elements.

These results clearly demonstrate that the influence of an input to an element (to cause bifurcation) is transferred not to faster but to slower elements.

4. Range of the time scale difference for the propagation

So far we have shown that for a range of τ, the change of one element is propagated not to faster but to slower elements. Here we quantitatively characterize the propagation, to see the range of (τ, L) explicitly.

In order to quantitatively estimate the change in the power spectra, we measure

$$\Delta_{i,1}(T_0) \equiv \left(\frac{1}{\log \omega_i^B - \log \omega_i^A} \int_{\log \omega_i^A}^{\log \omega_i^B} (\log P_i(\omega)|_{T_0} - \log P_i(\omega)|_0)^2 \, \mathrm{d} \log \omega \right)^{1/2}$$
$$= \left(\left(\log \frac{\omega_i^B}{\omega_i^A} \right)^{-1} \int_{\omega_i^A}^{\omega_i^B} \left(\log \frac{P_i(\omega)|_{T_0}}{P_i(\omega)|_0} \right)^2 \frac{\mathrm{d}\omega}{\omega} \right)^{1/2}, \tag{7}$$

where $P_i(\omega)|_0$ denotes the power spectrum of x_i without input at $i = 1$ and $P_i(\omega)|_{T_0}$ with $A \sin((2\pi t/T_0))$ applied at $i = 1$. This specific definition is not important. Any quantity characterizing the difference between two power spectra can be adopted. The region of the integration $\omega_i^A \leq \omega \leq \omega_i^B$ is near the time scale of each element T_i. $\Delta_{i,1}(T_0)$ expresses the difference of the dynamical property of $x_i(t)$, induced by the input $A \sin((2\pi t/T_0))$ at $i = 1$, by a measure on the frequency space near the time scale T_i. For example, it takes a large value in the shift of peak frequency or the bifurcation from limit cycle with sharp peak to chaos with broad peak, induced by the input

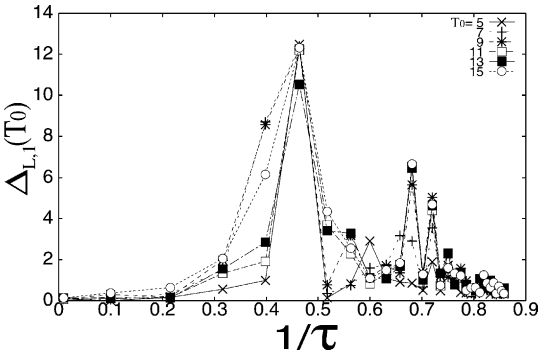

Fig. 8. The change in the power spectra at the slowest element, $\Delta_{L,1}(T_0)$, are plotted as a function of $1/\tau$. The marks correspond to the input periods. The change of the spectra is observed around $1.4 \lesssim \tau \lesssim 3.0$.

application. Fig. 8 shows $\Delta_{L,1}(T_0)$ are plotted as a function of $1/\tau$. As shown in Section 3.2, the change of the spectra is observed around $1.4 \lesssim \tau \lesssim 3.0$.

4.1. Larger T_{total} with τ = constant

Next we will show that the bifurcation cascade is maintained even if the total time scale difference T_{total} is much larger. Here we keep τ constant and increase the system size L so that $T_{\text{total}}(= \tau^{L-1})$ is larger. Fig. 9 shows the power spectrum of $x_i(t)$ with $\tau = 1.93$, i.e., under the same conditions as in Figs. 1(b) and 3(b), while L is chosen to be 20, and now $T_{\text{total}} = 2.7 \times 10^5$. Fig. 9(a) shows the spectra without any input while (b) shows the spectra at elements $i = 1, 10, 20$ without any input again (black line) and with the input $A \sin((t/T_0))$ applied at $i = 1$ (red line) ($T_0 = 1.5$). The common peaks among neighboring elements appear from high to low frequency region. These peaks are shifted dependent on the input. The difference between the spectra with and without input is maintained (or even amplified) down to the slowest element. As shown in Fig. 9(b), the spectra of the slowest element (the left figure) are changed after the input to the fastest element (the right one). (Compare the red line with the block line.) The input dependence appears even when the slowest element is 10^6 times slower than the fastest as shown in (b).

5. Bifurcation cascade

In Section 3, we have shown how fast elements affect slow dynamics. Successive transfer of bifurcation to slower elements gives a basis of the propagation of influence to slower elements, which we call the bifurcation cascade. The direction of the cascade was shown to be the opposite to that expected from the adiabatic approximation. Indeed, in the cascade process, coherence between the different time scales, is important, whereas such coherence is neglected in the adiabatic approximation. In this section, we study the conditions and the characteristic properties of the bifurcation cascade, as is commonly observed in the above examples as well as in some other models.

5.1. Conditions

We now study under what conditions the slower dynamics depends on the faster dynamics. Based on simulations of the present models for various parameters, the following three requirements are suggested.

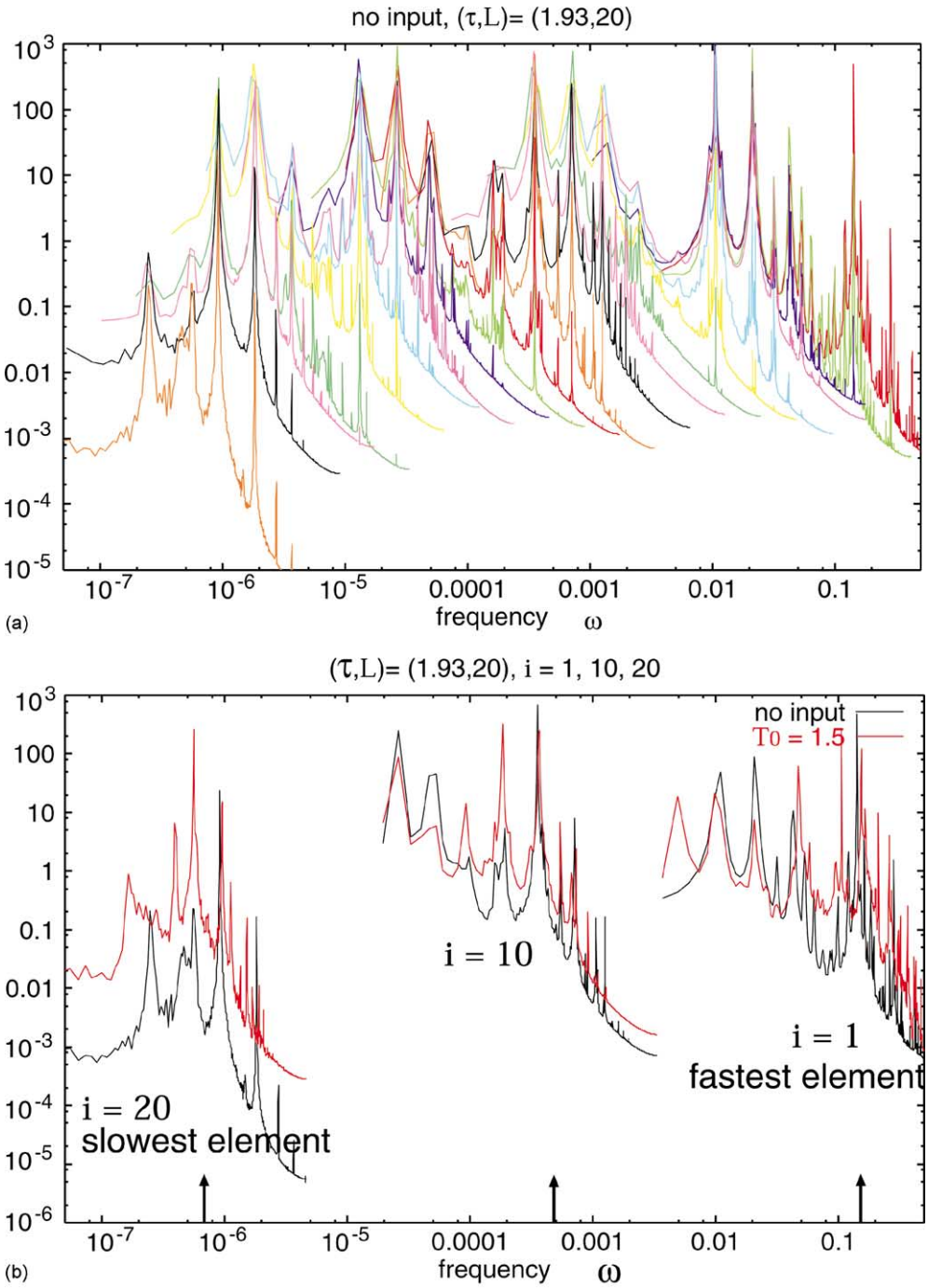

Fig. 9. Power spectrum for $x_i(t)$ with $(\tau, L) = (1.93, 20)$, i.e., $T_{\text{total}} = \tau^{L-1} = 2.7 \times 10^5$, where $A \sin(t/T_0)$ is applied at $i = 1$ ($T_0 \sim T_1$). (a) Spectra for each $x_i(t)$ where each element i is plotted with a different color and no input is applied. (b) The spectra with and without input ($A = 0.5$ and $T_0 = 1.5$) are shown by black and red lines, respectively. In (a) frequency locking are observed in the various scales as shown in Fig. 1(b). As can be seen, the difference between the black and red lines is apparent even for the slowest element. The arrows on the x-axis in (b) indicate the basic frequency of each element there is no coupling ($d = 0$).

Strong correlation. First, strong correlation, due to frequency locking between nearest neighbors in the chain is required, as can be seen, for example, in Fig. 1(b). When there is no such correlation, the adiabatic approximation for the faster dynamics is valid. For example, for large values of τ in Figs. 2 and 8, such coherence is not found, and the slower element is not influenced by the fastest element. For small values of τ, as is shown in Fig. 2(f), the degrees of freedom exhibiting chaotic instability per time scale is large due to the small time scale difference. Accordingly, the chaotic instability is so large that the bifurcation cascade is disturbed by the mixing property. Hence the cascade of bifurcations stops at some element with an intermediate time scale and cannot be propagated to the slowest element.

Existence of bifurcation. Second, the fastest dynamics is required to exhibit a bifurcation as the control parameter of the fastest element is changed. In our coupled Rössler equation, a bifurcation from a limit cycle to chaos is induced by the application of $A \sin(t/T_0)$ at $i = 1$. Such bifurcation is required to make switching to a different mode of dynamics possible.

However, this second condition by itself is not sufficient for the propagation of the bifurcated dynamics to slower elements since the control parameters of the slower element itself is not directly altered. Then, the transmission must occur through strong correlation described at the first condition. Furthermore, the change of dynamics must not damp through the propagation to much smaller elements, under the presence of the mixing property due to chaos. Now the next condition is required.

Marginal stability. To maintain correlation to distant elements, existence of a critical state is useful, since the correlation does not decay exponentially there. In the coupled Rössler equation, the marginally stable dynamics is required to guarantee the bifurcation cascade. For example, with $\tau = 1.93$ and $d = 0.45$ and $r = 1.4$, the dynamics are only weakly chaotic, as shown by the black dots in Fig. 4. There, some structure with collapsed tori or doubling of torus is discernible in Fig. 4 (see the black dots). The dynamics are near the onset of chaos, and marginally stability is sustained to all elements.[5] This is true whenever the propagation to the slowest element occurs. [6]

So far, in the present model we have chosen the same oscillators for each element with identical parameters r, d, and τ. However the bifurcation cascade is also expected to appear when this homogeneity is relaxed so that heterogeneous elements are employed which satisfy the above three conditions. For example, in a model with heterogeneous time scale variation, i.e., $T_i/T_{i-1} = \tau_i$, the bifurcation cascade appears if all τ_i are set within the range where the bifurcation cascade appears in the homogeneous time scale variation model described in Section 3.2.

Furthermore, to check the universality of the bifurcation cascade, we have also studied coupled Lorenz equations with different time scales, as will be reported [11]. There we have confirmed that the slowest element is influenced by the change of the fastest element, when the above three conditions are satisfied. In the case, again the bifurcation cascade is observed.

5.2. Origin of asymmetry

Here we discuss why the asymmetry in the propagation of the bifurcation cascade appears, with regard to the difference in time scales of the elements.

As shown in Section 3.4, there is an asymmetry in the propagation of the bifurcation cascade. One possible origin of this asymmetry lies in the chaotic dynamics itself.

[5] The marginal stability often allows for the coexistence of the (locally) chaotic dynamics and regular dynamics, similarly as chaotic itinerancy [7–10].

[6] A direct criterion for marginal stability is existence of null value(s) exponents characterizing instability, such as Lyapunov exponents. Here, however, the Lyapunov spectra are numerically difficult to measure, due to the huge difference in the time scales of the elements imposed by the power law time scale variation in our model.

For comparison, we have studied a coupled phase oscillator model without chaos, given by

$$T_i \frac{\mathrm{d}x_i}{\mathrm{d}t} = 1 - K \sin(x_i - x_{i+1}) - K \sin(x_i - x_{i-1}), \tag{8}$$

where $T_i = T_1 \tau^{i-1}$. We set K, τ such that the first condition described in Section 5.1 is satisfied. First we choose parameter values where chaos does not appear. In this case, we change only the K parameters of the fastest and the slowest elements. With this change, the dynamics of the next neighbor element can exhibit bifurcation. Depending on the magnitude of the parameter change, a bifurcation cascade may appear. In this case, however, the cascade propagates both from the slow to fast elements, and from the fast to slow elements. On the other hand, when the K, τ parameter values are chosen so that chaos appears while still preserving strong correlations between neighboring elements, the bifurcation cascade appears only in the one direction, from fast to slow elements [11].

Now, we propose the following conjecture as a possible origin of the asymmetry. Typically longer and longer time scales are involved in bifurcations from limit cycles to chaos. (Recall simply that chaos has "infinite period".) In most routes to chaos, for example, via the period doubling cascade or through n-dimensional torus, low frequency components appear along with the bifurcation to chaos. Higher frequency parts do not appear in general.

Therefore bifurcations change dynamics mostly in the low frequency region rather than in the high frequency region Now we revisit experiment shown in Fig. 7. Due to the application of the input at the intermediate element with $T_i = \sqrt{T_{\text{total}}}$, a bifurcation from chaos (black dots) to tori (blue dots) appears. According to the above discussion the frequency region with frequencies below inverse $\sqrt{T_{\text{total}}}$ should be influenced, while frequencies above that should not be strongly influenced. Therefore, the influence of the bifurcation on the neighboring elements will be felt more on the slower element than the faster element. This is the origin of the asymmetry.

Note that the bifurcation cascade can propagate up to very large time scale differences, T_{total}, as described in Section 4.1. If this type of cascade exists, biochemical reactions on subsecond time scales, for example, can affect dynamics on time scales as long as a day. This will be important when considering the generation of circadian rhythms and long term memory dynamics from intra-cellular reaction dynamics.

6. Discussion and conclusion

In conclusion, we have shown that in a system of coupled chaotic elements with time scales which are distributed according to a power law, the statistical properties of slower elements can be successively influenced by faster elements. This propagation of information is realized when there is: (i) strong correlation between neighboring elements such as frequency locking or anti-phase oscillation, (ii) a bifurcation in the dynamics of the fastest element as its control parameter is changed, and (iii) a cascade propagation of this bifurcation guaranteed by marginal stability. The mutual dependence of the elements in the chain is asymmetric in the sense that changes in the fastest elements can influence the slowest elements, but that changes in the slowest elements hardly ever influence the fastest elements. We note however that this asymmetry is in the opposite direction to the slaving principle [1] where the fast dynamics is irrelevant to the slow dynamics. The three requirements described here are found to be valid for the coupled Rössler equation and Lorenz equation.

We conjecture that these requirements generally give conditions for the transfer of correlation in the presence of chaos which amplifies the perturbation and can destroy the coherence. Although numerical calculations have been performed mainly for coupled Rössler equations, it is reasonable to expect that the propagation from faster to slower elements as described in this paper is a universal property of systems of coupled chaotic dynamical elements with distributed time scales, since the explanations given throughout the paper seem to be quite general. In fact, also in

the coupled Lorenz equations and coupled phase oscillators, such propagation can be observed and the above three requirements are found to be valid [11].

In chaotic dynamics, infinitely many modes are generated by nonlinearity, as shown in broad power spectra. Such modes are transferred to modes of the next element with a different time scale, though nonlinear coupling. In the present paper, we adopted $x_{i+1}z_i$ and $x_{i-1}z_i$ (Eq. (4)), with the same form of the nonlinearity in the Rössler equation, namely, xz in Eq. (3). On the other hand, if we adopt the nonlinear coupling such as $x_{i+1}x_i$ or $y_{i+1}y_i$ which a single Rössler equation does not contain, the bifurcation cascade cannot be observed. It seems that the mode coupling to the next element (with a different time scale) works better when the coupling has the same form as given in the (uncoupled) single element. Clarification of this point remains to be an important future problems.

Biological systems often incorporate multi time scale dynamics with changes on faster time scales sometimes influencing the dynamics on slower time scales leading to various forms of 'memory'. Cells can adapt to external conditions and maintain memory over long time spans through changes in their intra-cellular chemical dynamics. In neural systems, fast changes in the input can be kept as memory over much longer time scales when short-term memories are fixed to long-term memories (for a viewpoint on dynamic memory, see [9,12]). In a similar way, a recently proposed dynamical systems theory of evolution proposes the fixation of phenotypic change (by bifurcation) to slower genetic change [13].

This mechanism for the propagation of bifurcations from faster to slower elements will be relevant for the study of such kinds of biological system, and it will be interesting to find out whether the three conditions on the dynamics that we proposed are satisfied as well. In physics, the possibility of influencing the slower dynamics by controlling the faster elements through a cascade process will be important for the control of turbulence in general.

Acknowledgements

The authors would like to thank S. Sasa, T. Ikegami, T. Shibata, H. Chatè, M. Sano, I. Tsuda, T. Yanagita, Y.Y. Yamaguchi, M. Toda, Y. Kuramoto for discussions. They are also grateful to A. Ponzi, F. Willeboordse for critical reading of the manuscript. This work is partially supported by grants-in-aid for Scientific Research from the Ministry of Education, Science, and Culture of Japan (11CE2006).

Appendix A. Another example for coupled Rössler equations

We have studied some models with nonlinear coupling terms without divergence. An example for a coupled Rössler equation, introduced by Eq. (4), is given by

$$\mathbf{D^d} = \begin{bmatrix} 0 & -0.4 & -0.3 \\ 0.3 & 0.4a & 0 \\ 0.3b & 0 & 0.3r \end{bmatrix}, \qquad d_2^n = d_1^n, \qquad d_3^n = (d_1^n)^2. \tag{A.1}$$

There are nonlinear coupling terms z_ix_{i+1}, z_ix_{i-1}, x_iz_{i+1}, x_iz_{i-1}, $z_{i+1}x_{i+1}$, $z_{i+1}x_{i-1}$, $z_{i-1}x_{i+1}$, and $z_{i-1}x_{i-1}$.[7] The phenomena reported in the present paper are again observed in a wide range of the coupling strength, namely, $d_1^n \geq 0.38$ under $(\tau, L) = (1.93, 8)$ and $r = 1.4$ in Eqs. (4) and (A.1).

Of course, the behavior of the models in the present paper is observed over some range of the coupling parameters, $\mathbf{D^d}$, d_1^n, d_2^n and d_3^n.

[7] Such types of the coupling as $x_{i+1}z_{i-1}$ are also adopted in the shell model [2].

References

[1] H. Haken, Synergetics, Springer, Berlin, 1977.
[2] M. Yamada, K. Ohkitani, Phys. Rev. Lett. 60 (1988) 983.
[3] E.N. Lorenz, J. Atoms. Sci. 20 (1963) 130–141.
[4] J.B. Maclaulin, P.C. Martin, Phys. Rev. A. 12 (1975) 186–203.
[5] A.T. Winfree, Geometry of Biological Time, Springer, Berlin, 1980.
[6] Y. Kuramoto, Chemical Oscillation, Waves, and Turbulence, Springer, Berlin, 1984.
[7] K. Kaneko, Physica D 41 (1990) 137.
[8] K. Ikeda, K. Matsumoto, K. Otsuka, Prog. Theor. Phys. Suppl. 99 (1989) 295–324.
[9] I. Tsuda, Neural Networks 5 (1992) 313.
[10] K. Kaneko, Physica D 77 (1994) 456.
[11] K. Fujimoto, K. Kaneko, submitted to Chaos.
[12] A. Skarda, W.J. Freeman, Behav. Brain Sci. 10 (1987) 161–173.
[13] K. Kaneko, T. Yomo, Proc. Roy. Soc. Lond. B 267 (2000) 2367–2373;
K. Kaneko, T. Yomo, Evol. Ecol. Res. 4 (2002) 317–350.